Photophysics of Soret-Excited Tetrapyrroles in Solution. II. Effects of Perdeuteration, Substituent Nature and Position, and Macrocycle Structure and Conformation in Zinc(II) Porphyrins

Xia Liu,[†] Umakanta Tripathy,[†] Sheshanath V. Bhosale,[‡] Steven J. Langford,[‡] and Ronald P. Steer*,[†]

Department of Chemistry, University of Saskatchewan, 110 Science Place Saskatoon, SK Canada S7N 5C9, and School of Chemistry, Monash University, Wellington Road, Clayton VIC 3800, Australia

Received: May 30, 2008; Revised Manuscript Received: July 11, 2008

The steady-state absorption, fluorescence, and excitation spectra and upper excited-state temporal fluorescence decay profiles of 11 tetrapyrroles in several fluid solvents are presented and analyzed to ascertain the factors that control their S_2 population decay times. The S_2 lifetimes, which vary by more than 2 orders of magnitude, are controlled exclusively by their rates of radiationless decay. The only important electronic relaxation path is S_2-S_1 internal conversion, the efficiency of which is near 1.0 in all compounds studied (except CdTPP where it is 0.69). The rate of S_1 population rise equals the rate of S_2 population decay in all cases. Among the compounds studied, only MgTPP exhibits S_2-S_1 decay behavior that corresponds to the weak coupling limit of radiationless transition theory; all zinc metalloporphyrins exhibit intermediate to strong coupling. Perdeuteration of ZnTPP produces no significant change in the rate of S_2 decay or in the quantum yield of S_2-S_0 fluorescence, indicating that in-plane C−C and C−N vibrations are the accepting modes in S_1 with the largest Franck−Condon factors. The initial vibrational energy content of the S_2 states ($0 < E_{vib} < 3500$ cm^{-1} over the range of compounds) plays no significant role in determining their overall population decay rates in solution. The S_2 population decay rates of these tetrapyrroles are controlled by two factors: the Franck−Condon factor, which is inversely proportional to the exponent of the S_2-S_1 electronic energy spacing and the S_2-S_1 coupling energy. The S_2-S_1 electronic energy spacing is determined in solution by the difference in the polarizabilities of the S_2 and S_1 states and can be controlled by varying the polarizability of the solvent. The S_2-S_1 coupling energy is influenced by the nature, location, and effect of the substituents, with β-alkyl substitution and reduction of symmetry in the tetrapyrrole—for example by loss of planarity—increasing the interstate coupling energy.

Introduction

Tetrapyrroles and their metallated derivatives are ubiquitous in nature. The unique spectroscopic, photophysical, and photochemical properties of this large family of compounds have also resulted in their use in photon-activated applications as diverse as organic solar photovoltaic cells,[1] photodynamic therapy,[2] oxygen sensors,[3] and molecular electronics.[4] Investigations of the structure−function relationships of these families of compounds over several decades have produced a wealth of information about the photophysical and photochemical behavior of their lowest triplet and lowest excited singlet states both in monochromophoric and polychromophoric systems.[5] Surprisingly, however, fundamental questions regarding the relationships between their structure and the chemical and physical behavior of the higher excited electronic states that are accessed by photon absorption in their strong Soret bands remain open.[6]

The lifetimes of the higher excited singlet states produced upon Soret-band excitation of the tetrapyrroles in dilute solution are determined by their rates of intramolecular radiationless relaxation. Although the photophysical behavior of the higher excited states of individual molecules and small sets of related tetrapyrolles have been reported,[6] no comprehensive analysis of the structure excited-state properties of the group as a whole is yet available. We are attempting to remedy this deficiency for the diamagnetic d^0 and d^{10} metallated tetrapyrroles, a set of compounds chosen to avoid complications due to axial ligation and the presence of charge transfer and d−d excited states present in open d-shell species.[7,8]

Part I of this series of papers[9] described experiments to examine the dynamics and mechanism(s) of the relaxation, following excitation in their Soret (S_2-S_0) absorption bands, of the meso-substituted 5,10,15,20-tetraphenylmetalloporphyrins, MTPP (M = Mg, Zn, Cd). The nonradiative decay of the S_2 state of MgTPP involves internal conversion to S_1 with unit efficiency at rates that conform well to the weak S_2-S_1 coupling limit of radiationless transition theory.[10] However, the corresponding S_2 states of CdTPP and even the model compound ZnTPP exhibit decay rates that are faster than those predicted in the weak coupling limit. A small fraction of the S_2 population of ZnTPP (ca. 7%) and about 30% of the S_2 population of CdTPP decay by a process that bypasses the S_1 state. This dark decay pathway may be S_2-T_n ($n > 2$) intersystem crossing, direct relaxation to S_0, or indirect relaxation via a nearby gerade excited singlet state. However, this minor process cannot account for the greatly enhanced rates of S_2-S_1 internal conversion in these compounds relative to MgTPP. At the other extreme, the rates of radiationless decay of the S_2 states of simple β-substituted metalloporphyrins such as ZnOEP occur at macrocycle

* To whom correspondence should be addressed. Phone: (306) 966-4667. Fax. (306) 966-4730. Email: ron.steer@usask.ca.
[†] University of Saskatchewan.
[‡] Monash University.

10.1021/jp804792x CCC: $40.75
Published on Web 08/28/2008

CHART 1: Structures

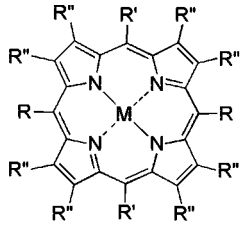

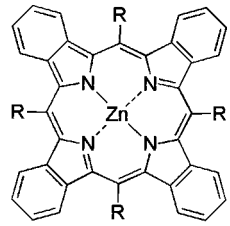

ZnP, M = Zn; R = R' = R" = H
ZnDPP, M = Zn; R = Ph; R' = R" = H
MTPP, M = Zn; Mg, Cd; R = R' = Ph; R" = H
TPP-d_{30}, M = 2D; R = R' = C_6D_5; R" = D
ZnTPP-d_{28}, M = Zn; R = R' = C_6D_5; R" = D
ZnOEP, M = Zn; R = R' = H; R" = Et
ZnTPP(F_{20}), M = Zn; R = R' = C_6F_5; R" = H
ZnTPP(Cl_8), M = Zn; R" = H; R = R' =

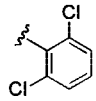

ZnTBP, R = H
ZnTPTBP, R = Ph

ring stretching frequencies and fall squarely within the strong S_2-S_1 coupling regime.

The following questions remain open. (i) What is the fundamental source of the range of S_2-S_1 interstate coupling energies (from weak to strong) among the simple meso- and β-substituted d^0 or d^{10} metalloporphyrins? (ii) Is there a fundamental difference between meso- and β-substitution? (iii) There is both computational[11] and experimental[12,13] evidence for the presence of at least one dark state (S_2' of perhaps gerade parity) that lies near in energy to the S_2 (2^1E_u) state in ZnTPP. Does such a state (or states) influence the radiationless decay dynamics of the S_2 states of the d^0 and d^{10} metalloporphyrins generally? (iv) What is the effect on the S_2 relaxation dynamics of changes in the symmetry of the metalloporphyrin macrocycle brought about by ring fusion, by the pattern of substitution, and by distortion of the tetrapyrrole or metallo-tetrapyrrole structure? A brief report of the lifetime of the S_2 state of a zinc diaryllporphyrin with D_{2h} symmetry is available,[14] but there has been no systematic study of the effect of changes in substitutional symmetry on the S_2 decay dynamics of tetrapyrroles. (v) Various halogenated, alkylated, sufonated, and otherwise substituted phenyl groups have been used to impart desirable properties to the ground states of the metalloporphyrins. What influence do these phenyl-ring substituents have on the excited-state decay dynamics? (vi) Finally, can a predictive relationship be developed between the measurable steady-state spectroscopic properties of the tetrapyrroles and their rates of S_2 excited-state relaxation?

We seek to answer these questions by examining the spectroscopic and photophysical properties of the following Soret-excited porphyrins: ZnTPP and its per-deuterated analogue, zinc(II) porphine (ZnP), zinc(II) 5,15-diphenylporphyrin (ZnDPP), zinc(II) tetrabenzoporphyrin (ZnTBP), zinc(II) 5,10,15,20-tetraphenyltetrabenzo-porphyrin (ZnTPTBP), and two halogenated analogues of ZnTPP, zinc(II) 5,10,15,20-tetrakis(pentafluorophenyl)porphyrin and zinc(II) 5,10,15,20-tetrakis(2,6-dichloro-phenyl)porphyrin (ZnTPP(F_{20}) and ZnTPP(Cl_8), Chart 1). A comprehensive analysis of the factors controlling the rates of S_2 radiationless relaxation in these and other diamagnetic metalloporphyrins is undertaken.

Experimental Methods

(i) Materials. MgTPP, ZnTPP, CdTPP, ZnP, H_2TPP, ZnTPP(F_{20}), ZnTPP(Cl_8), and ZnTPTBP were all purchased from Frontier Scientific, contained no impurities that fluoresced significantly in the Soret region, and were used as received. TPP-d_{30}, ZnTPP-d_{28}, and ZnDPP were all synthesized de novo and were purified to remove persistent fluorescent impurities. The general conditions used for these syntheses and purifications are outlined below. Details are given in the Supporting Information. Solvents were purchased from Sigma-Aldrich and were used as received.

Synthesis reagents including solvents were used as purchased. UV−visible spectra were recorded on a Varian model Cary 100 Bio UV−visible spectrophotometer, with the solvent systems used stated in the synthesis description. ^{1}H and ^{13}C nuclear magnetic resonance (NMR) spectra were recorded by using a Bruker DPX 300 MHz spectrometer (300 MHz ^{1}H, 75 MHz ^{13}C) or a Bruker DRX 400 MHz spectrometer (400 MHz ^{1}H, 100 MHz ^{13}C), as solutions in the deuterated solvents specified in the Supporting Information. Deuterated chloroform ($CDCl_3$) was stored over anhydrous Na_2CO_3 and was filtered prior to use. Low-resolution electrospray mass spectra (LR-MS) were recorded on a Micromass Platform API QMS-quadrupole electrospray mass spectrometer.

The purification of ZnTBP was particularly problematic. The material purchased from Sigma-Aldrich has a dye content of 80% and contains a strongly fluorescent impurity detectable by UV−visible absorption spectroscopy at 460 nm. The detailed method of purifying ZnTBP is given in the Supporting Information.

(ii) Instrumentation and Instrumental Methods. The instrumentation and procedures used for steady state and fluorescence upconversion experiments have been described in detail elsewhere.[9] In the present work, the temporal resolution of the fluorescence upconversion system was improved by employing smaller step sizes in the gate pulse delay line ($\Delta t = 3.3n$ ($n = 1, 2, ..., 20$) fs) in order to describe the instrument response function and the temporal fluorescence profiles of the short-lived states with a larger and more statistically significant number of data points. The fluorescence decay constants were then extracted by convoluting trial decay functions with the instrument response function and obtaining the parameters of the convoluted function that minimized the sum of the squares of the deviations between it and the measured decay as described previously.[9] We estimate that the uncertainty in the measurement of the Soret-excited (S_2) fluorescence lifetimes is ±30 fs with this improvement in place.

Steady-state absorption spectra were measured on a Varian-Cary 500 spectrophotometer. Fluorescence spectra were measured with either a Jobin-Yvon Spex Fluorolog or a Photon Technology Intenational QuantaMaster spectrofluorometer, both of which were fitted with double excitation and emission monochromators.

(iii) Fluorometry Methods. Emission spectra were corrected synchronously by using detector/monochromator sensitivity files supplied by the manufacturers. Particular care was needed to obtain fully corrected S_2-S_0 emission spectra when the emission quantum yields were very small. First, the solvent background, predominately Raman scatter, was corrected before subtraction from the measured fluorescence (plus background) spectrum by multiplying it by the constant correction factor $F = (1 - 10^{-A_{ex}})/2.303A_{ex}$, where A_{ex} is the absorbance of the sample solution in the same solvent at the sample excitation wavelength. This serves to correct the measured background for the reduced intensity of incident light traversing the cell when it contains the sample solution as compared with pure solvent. Correction for reabsorption of the S_2-S_0 emission by the strong Soret

TABLE 1: Steady-State Spectroscopic Data[a]

compound/ solvent	$E^{0-0}(S_2)$ (cm^{-1})	$\varepsilon_S^{max}/10^5$ ($M^{-1}cm^{-1}$)	$fwhm_S$ (cm^{-1})	$\varepsilon_{S(1-0)}/\varepsilon_{S(0-0)}$	SS (S_2) (cm^{-1})	$E^{0-0}(S_1)$ (cm^{-1})	$\varepsilon_Q^{max}/10^4$ (cm^{-1})	$fwhm_Q$ (cm^{-1})	SS (S_1) (cm^{-1})	$\varepsilon_{(1-0)}/\varepsilon_{(0-0)}$	$f_Q/(f_B + f_Q)$	ΔE (S_2S_1) (cm^{-1})
						MgTPP						
Ethanol	23700		370	0.064	120	16630		370	80	1.59	0.083	7070
C_6H_5F	23500		450	0.077	190	16600		380	100	2.12	0.063	6900
Benzene	23420	5.36	450	0.064	160	16540	1.8	430	160	1.91	0.060	6880
Toluene	23350	5.74	540	0.074	200	16540	1.9	420	160	2.40	0.058	6910
CS_2	22830	3.90	660	0.065		16420	2.1	450	130	2.10	0.078	6410
						ZnTPP[b]						
Ethanol	23620	6.58	320	0.07	140	16690	2.17	400	200	2.88	0.056	6930
DMF	23470	7.29	490	0.07	120	16640	2.36	410	180	2.29	0.060	6830
Benzene	23560	5.87	690	0.07	170	16870	2.54	460	250	5.92	0.058	6695
						ZnTPP-d_{28}						
Ethanol	23650	6.58		0.07	150	16730	2.17	360	150	2.89	0.054	6920
Benzene	23600	5.87	630	0.07	250	16890	2.54	450	290	5.86	0.061	6710
						ZnTPP(F_{20})						
Ethanol	23800	5.52	500	0.106	270	16970	2.51	450	230	8.8	0.052	6830
						ZnTPP(Cl_8)						
Ethanol	23450	5.70	270	0.076	190	16860	2.24	510		13.2	0.059	6590
						CdTPP						
Ethanol	23160	5.41	560	0.11	187	16280	2.02	420	249	1.45	0.054	6880
Benzene	22910		750	0.15	288	16210		570	684	1.75	0.059	6800
						ZnP						
Ethanol	25070	3.8	440	0.094	100	17630	1.34	360	138	4.41	0.051	7440
						ZnDPP						
Ethanol	24260	6.11	470	0.08	188	17130	1.99	320	170	5.95	0.057	7130
DMF	24130		510	0.08	217	17090		380	190	5.55	0.053	7040
Benzene[c]	24150			0.08	190						0.057	6711
						ZnTBP						
Ethanol	23640		390	0.12	112	16040	4.14	250	51	0.08	0.149	7600
DMF	23430		590	0.12	110	15980		260	58	0.06	0.157	7450
Pyridine	23050		650	0.12		15880		300		0.11	0.162	7170
						ZnTPTBP[c]						
Ethanol	21700	3.4	840	0.12		15360	5.64	460	192	0.30	0.108	6190
DMF	21210		940	0.13		15160		480	263	0.39	0.119	6050
Benzene	21200		1120	0.12		15230		440	110	0.27	0.127	5970
Pyridine	20880		880	0.11		15070		460	304	0.43	0.124	5810
						ZnOEP[c]						
Ethanol	24570	3.73	510	0.15		17440	2.01	350		0.90	0.076	7130
Toluene	24720	4.17	750	0.15		17560	3.94	340		0.55	0.078	7160

[a] Wavenumbers quoted to nearest 10. [b] Additional data for ZnTPP may be found in ref 9. [c] Wavenumbers from the maxima of the origins of the Q and B bands in the absorption spectra.

absorption band was minimized by employing dilute sample solutions and sample cells with short emission path lengths (e.g., 10 mm × 2 mm with emission viewed along the short path). When comparing fluorescence excitation and absorption spectra, care was taken to ensure that both were measured with the same excitation and emission bandwidths (typically, 1.8 or 2.0 nm). The excitation spectra were corrected by viewing the sampled excitation light with a calibrated photodiode and dividing the raw excitation intensity by the resulting signal. Artifacts resulting from changes in the excitation intensity at the viewed emissive volume due to the finite absorbance of the solution (especially important when scanning through the strong Soret absorption band) were minimized by using cells with short excitation paths (e.g., 2 mm × 10 mm with emission viewed along the long path).

Fluorescence quantum yields were measured as described in detail previously,[12] by using ZnTPP in ethanol as a standard ($c = 5 \times 10^{-7}$ M, $\phi_f = 1.42 \times 10^{-3}$ at $\lambda_{ex} = 400$ nm) and correcting for differences in solvent refractive index when necessary. In a few cases (e.g., ZnP), the same excitation wavelength could not be used for both sample and reference. In these cases, the measured quantum yields were corrected to equal excitation photon flux by using a calibrated photodiode that sampled the incident intensities at the two excitation wavelengths.

All measurements were made at room temperature.

(iv) DFT Calculations. DFT calculations on ZnDPP were performed as described in detail for ZnTPP in ref 11. Briefly, the calculations were carried out with the B3LYP hybrid functional by using the Gaussian 03W program. For the MTPP series, ground-state geometries were calculated by using three different basis sets, 6-31G(d), lanl2dz, and CEP-31G, all of which yielded similar structures. Thereafter, calculations for other zinc(II) porphyrins were performed with only the 6-31G(d) basis set. Excitation energies and oscillator strengths were then obtained by TDDFT calculations at the B3LYP level by using the 6-31G(d) basis set and the ground-state optimized structures obtained with it.

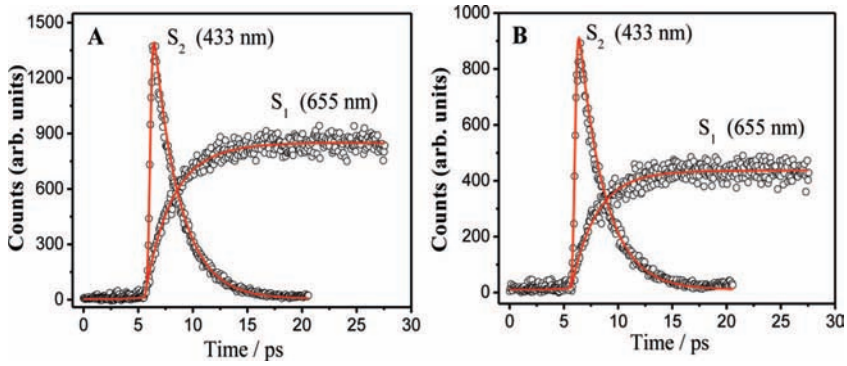

Figure 1. Temporal S_2 and S_1 fluorescence upconversion profiles of (a) ZnTPP in ethanol ($\tau(S_2) = 2.35$ ps; $\tau(S_1$ rise$) = 2.34$ ps) and (b) ZnTPP-d_{28} in ethanol ($\tau(S_2) = 2.36$ ps; $\tau(S_1$ rise$) = 2.34$ ps). Measurements are at room temperature with $\lambda_{ex} = 400$ nm, and central observation wavelength is shown. The solid lines give the best fits of single-exponential decay and rise functions to the measured data.

Results and Discussion

We shall organize the results and discussion section of this paper by first presenting the results of steady-state spectroscopy experiments common to all of the compounds investigated. We shall then present the results of dynamics experiments designed to provide comparisons among related subsets of the tetrapyrroles. Finally, a global analysis of the complete set of results is presented and discussed.

(i) Steady-State Spectroscopy. The results of steady-state absorption, fluorescence emission, and excitation experiments are presented in Table 1. The absorption and emission spectra of most of these compounds have been previously reported by us and by others;[5,6] in all such cases, our spectra do not differ materially from those in the literature. Representative spectra are provided in the Supporting Information that accompanies this paper. Data such as the Stokes shifts and the relative intensities and widths of resolved vibrational features in these spectra have been acquired under identical conditions of spectral bandwidth, and so forth, to facilitate comparisons among them.

The data in Table 1 reveal several solvatochromic effects common to all of the zinc metalloporphyrins investigated. The main effect is a bathochromic shift in both the Q and B bands that increases with increasing solvent polarizability. The B band is more sensitive than is the Q-band, with the result that the electronic energy spacing, $\Delta E(S_2-S_1)$, decreases with increasing refractive index (and polarizability) of the solvent. The relative intensities and widths of the resolvable vibronic features in the absorption and emission spectra are strong functions of the porphyrin structure but only weak functions of solvent. The effects of incomplete axial coordination of the metalloporphyrin can be seen in some coordinating solvents (e.g., MgTPP in DMF), as previously documented by others.[7] In these cases, the overlapping vibronic bands attributed to species having different coordination are resolved by modeling the observed spectra (on a wavenumber scale) by a sum of Gaussian functions.

In all cases investigated here, the corrected fluorescence excitation spectra are almost identical to the absorption spectra. Three kinds of fluorescence excitation spectra were acquired. First, for every solute/solvent system investigated here, the corrected normalized fluorescence excitation spectrum obtained by exciting in the Q-band and observing emission further to the red in the S_1-S_0 fluorescence band system reproduced the Q-band absorption spectrum, as has previously been reported.[9] Second, the corrected and separately normalized fluorescence excitation spectrum obtained by exciting in the B band and observing emission in the S_1-S_0 fluorescence band system was almost identical to the B band absorption spectrum, in each system. These observations confirm our previous conclusion[9,11] that any effects on the pathway and net internal conversion efficiency of the decay of the S_2 state that might be associated with a changing vibrational energy as the excitation wavelength changes within the B band are either minor or not revealed in the steady-state spectra. Third, the corrected fluorescence excitation spectra obtained by observing Q-band emission, exciting over the whole of the Q- and B-band absorption range, and normalizing only the Q-band excitation spectrum with the Q-band absorption spectrum showed that the corrected excitation spectrum in the B-band region matched the B-band absorption spectrum well in both shape and intensity. The integrated intensity of the B−X excitation spectrum obtained in this way was never less than 90% of that of the B−X absorption spectrum in all zinc metalloporphyrins in all the solvents investigated. Thus, the efficiency of S_2-S_1 internal conversion, η_{ICS2}, must lie in the range $0.9 \leq \eta_{ICS2} \leq 1.0$ in all systems investigated here, irrespectively of the 2 orders of magnitude range in the measured rates of this process over the whole set of compounds.

The S_2-S_0 fluorescence spectra ranged in intensity from weak ($\phi_f \approx 10^{-3}$) to extremely weak ($\phi_f \approx 10^{-6}$), but all were measurable, albeit with varying signal-to-noise, because the oscillator strength of the radiative Soret transition is so large ($f \approx 1$). The background signal, primarily solvent Raman scatter, was scaled before subtracting it from the sample spectrum to account for excitation intensity differences in the solution and pure solvent as described in detail above. Further correction of these spectra for fluorescence reabsorption was minimized by employing very dilute solutions and cells with short emission pathlengths. Such precautions allowed us to obtain reliably reproducible S_2 emission spectra and quantum yields in all cases except ZnOEP (for which $\phi_f \approx 10^{-6}$). For this compound alone, a higher concentration of solute and front-face illumination in a triangular cell were necessary to obtain a measurable steady-state emission spectrum. Because only modest signal-to-noise could be obtained in these corrected S_2-S_0 fluorescence spectra, the Stokes shifts and widths of the emission bands and the fluorescence quantum yields could be measured with relatively small error only in the most highly fluorescent samples (e.g., ZnTPP), with the absolute error in these quantities increasing with decreasing fluorescence quantum yield.

In Table 1, the relative intensities of the 0−0 and 1−0 vibronic features in the Q and B absorption systems were obtained from the relative absorbances at the peak maxima. The fraction of the overall Q + B band intensity attributable to the Q band, $f_Q/(f_Q + f_B)$, was obtained by measuring the integrated

TABLE 2: Dynamics Data

compound/solvent	f_l	$\Delta E(S_2-S_1)$ (cm^{-1})	$\phi_f/10^{-3}$	τ_{S1} rise (ps)	τ_{S2} (ps)	$k_r/10^8$ (s^{-1})	$k_{nr}/10^{11}$ (s^{-1})	C^a (cm^{-1})
			MgTPP					76
Ethanol	0.222	7103	2.4	3.25	3.28	7.3	3.05	
C_6H_5F	0.276	6910	2.4		2.82	8.5	3.55	
Benzene	0.295	6893	2.5	2.69	2.71	9.2	3.69	
Toluene	0.296	6880	2.3		2.55	9.0	3.92	
			ZnTPP					81
Ethanol	0.222	6930	1.42	2.34	2.35	6.04	4.26	
DMF	0.257	6832	1.50	2.07	2.15	6.98	4.65	
Benzene	0.295	6695	1.14	1.41	1.49	7.65	6.71	
			ZnTPP-d_{28}					80
Ethanol	0.222	6922	1.5	2.34	2.36	6.4	4.24	
Benzene	0.295	6713		1.49	1.50		6.67	
			ZnTPP(F_{20})					183
Ethanol	0.222	6828	0.19	0.45	0.46	4.0	22	
			ZnTPP(Cl_8)					98
Ethanol	0.222	6671	0.88	1.34	1.36	6.5	7.35	
			CdTPP					197
Ethanol	0.222	6875	0.138	0.30	0.31	4.5	32	
Benzene	0.295	6696	0.129	0.24	0.24	5.4	42	
			ZnP					173
Ethanol	0.222	7445	0.42	0.90	0.91	4.6	11.0	
			ZnDPP					85
Ethanol	0.222	7129	1.61	2.31	2.30	7.00	4.35	
DMF	0.257	7033	1.50	2.00	2.01	7.46	4.98	
Benzene	0.295	6711	1.67	1.78	1.79	9.33	5.59	
			ZnTBP					136
Ethanol	0.222	7601			1.30		7.69	
DMF	0.257	7447	2.37		2.55	9.29	3.92	
Benzene	0.295	7487			1.01		9.90	
Pyridine	0.300	7169		1.51	1.53		6.54	
			ZnTPTBP					87
Ethanol	0.222	6189	0.79	0.93	0.93	8.5	10.8	
DMF	0.257	6047	1.22	0.74	0.75	16	13.3	
Benzene	0.295	5962	1.43	0.68	0.68	21	14.7	
Pyridine	0.300	5810		0.43	0.43		23	
			ZnOEP					2000[b]
Ethanol	0.222	7133	~0.001	<0.05	<0.05		>200	

[a] Calculated for data in ethanol. [b] Best estimate based on $\tau(S_2) = 24$ fs (see text).

areas under the full Q- and B-band absorption systems, that is, $f \propto \int \varepsilon(\bar{\nu})\, d\bar{\nu}$.

(ii) Effects of Deuteration. Our previous analysis[9] of the rates of S_2 decay of MgTPP as a function of solvatochromically induced variations in its S_2-S_1 electronic energy spacing revealed that S_2-S_1 interstate interactions in this molecule conform to the weak coupling case of radiationless transition theory, and that multiple in-plane C−C and C−N stretching vibrations are the main accepting modes in the lower state. ZnTPP was shown to exhibit S_2-S_1 radiationless transition rates that increased faster with decreasing energy gap than permitted in the weak coupling regime. In order to examine whether C−H stretching vibrations mediate S_2-S_1 coupling in any way, both the perdeuterated free-base meso-substituted tetraphenylporphyrin and ZnTPP were synthesized (yielding TPP-d_{30} and ZnTPP-d_{28} in >98% isotopic purity), and their S_2 emission lifetimes and fluorescence spectra were compared with those of the undeuterated compounds.

The results of fs fluorescence upconversion experiments on ZnTPP and ZnTPP-d_{28} are shown in Figure 1. For each compound in the same solvent, the S_2 temporal fluorescence decay profile is well described by a single-exponential function and has a decay constant equal to its S_1 fluorescence risetime within an experimental error of ca. 50 fs. Deuteration has no measurable effect on either lifetime. The results are summarized in Table 2.

In the weak coupling limit, the effect of perdeuteration of an organic molecule on its radiationless transition rates is associated with reductions in the Franck−Condon factors for the vibrations, often C−H stretches, that are most effective in coupling the two states. Equations 1 and 2 are the analytical expressions developed by Englman and Jortner[10] to describe the effect of deuteration in the weak coupling limit:

$$k_{nr} = \{\sqrt{2\pi}C^2/\hbar(\hbar\omega_M\Delta E)^{1/2}\}\exp\{-(\gamma/\hbar\omega_M)\Delta E\} \quad (1)$$

where $\gamma = \ln\{2\Delta E/\sum_M \hbar\omega_M\Delta_M^2\} - 1$ and

$$\frac{k_H}{k_D} = \left(\frac{\hbar\omega_D}{\hbar\omega_H}\right)^{1/2}\exp\left\{\gamma\Delta E\left(\frac{1}{\hbar\omega_D} - \frac{1}{\hbar\omega_H}\right)\right\} \quad (2)$$

Here, k_H and k_D are the nonradiative transition rate constants for the perhydro and perdeutero species, $\hbar\omega_H$ and $\hbar\omega_D$ are the frequencies of the vibrations under consideration, ΔE is the electronic energy spacing between the two coupled states, and γ is a function of the dimensionless displacement parameter, Δ_M, and the degeneracy (or near degeneracy when taken as the

number of vibrations in the above sum), d_M, of the accepting vibrational mode(s). The values of the interstate coupling energy, C, are taken to be the same in both the perhydro and perdeutero species. By using the values of γ obtained from the energy gap law plots[9] for MgTPP and ZnTPP, one estimates, by using eq 1, that perdeuteration of either ZnTPP or H_2TPP should slow the rate of S_2-S_1 internal conversion by a factor of ≥ 2.2 at $\Delta E = 7000$ cm^{-1} if C−H(D) stretches are the dominant accepting modes in the radiationless transition.

Such a variation in S_2 fluorescence lifetime would easily have been measurable upon perdeuteration of ZnTPP, but no significant difference was observed in the experimental lifetimes, confirming that C−H(D) vibrations are not directly involved in S_2-S_1 vibronic coupling in this model metalloporphyrin. If instead, C−C and C−N stretching vibrations of the macrocycle act as accepting modes, the effect of perdeuteration will be small but nevertheless finite. Estimating that perdeuteration at the eight β positions of ZnTPP would decrease the average frequency of in-plane C−C(N) stretching vibrations in the macrocycle by ≤4%, one predicts that the value of k_H/k_D should lie in the range $1.00 \leq k_H/k_D \leq 1.03$. In fact, careful measurement of the S_2-S_0 fluorescence spectra of dilute solutions of ZnTPP and ZnTPP-d_{28} in ethanol, excited under exactly the same set of instrumental conditions and corrected for small differences in absorbance at the excitation wavelength, reveals a very slight increase—estimated to be ca. 3%—in the radiative yield from the perdeuterated species. A secondary deuterium isotope effect of such a magnitude is completely consistent with the above analysis; multiple ($d_M > 20$) in-plane C−C(N) stretching vibrations of the macrocycle, most of which lie in the 1200−1600 cm^{-1} range,[15] are the accepting modes in the S_2-S_1 transition. (The use of ground-state frequencies[15] in this analysis assumes that the frequencies are not substantially reduced in the excited state.)

For the free-base tetraphenylporphyrin, one should consider the possibility not only that N−H(D) vibrations might act as accepting modes but also that a primary deuterium isotope effect might affect the rate of any process involving radiationless decay via a displacement along the path leading to interconversion, by tunneling, of its tautomeric structures (i.e., H(D) atoms on the N atoms exchanging position). For the latter process, comparing H_2TPP with D_2TPP, the isotope effect would be expected to be considerably larger than that associated with the variation in Franck−Condon factors, involving, as it must, larger amplitude atom displacements associated, in the limit, with bond scission/formation.

The lifetime of the Soret-excited (B) state of H_2TPP in condensed media is very short. Vacha et al.[16] estimate its excited-state lifetime to be 82 fs from homogeneous hole burning in PMMA at 20 K; Zhong, et al.[17] estimate ca. 20 fs in chloroform at room temperature by using a fluorescence depletion method, and Baskin, Yu, and Zewail (BYZ)[18] measure $\tau \leq 50$ fs in benzene by fluorescence upconversion. To account for the reduction in the lifetime of H_2TPP compared with ZnTPP, BYZ invoked an energy gap law argument based on (i) weak coupling of the B and Q_y states at the smaller electronic energy gap, $\Delta E(B-Q_y) = 5650$ cm^{-1}, and (ii) an acceleration of the relaxation rate by excess vibrational energy deposited in the molecule when exciting to the blue of the Soret band origin. With the temporal resolution of our present fluorescence upconversion instrumentation, we would be unable to distinguish differences between the B-band fluorescence lifetimes of H_2TPP and TPP-d_{30} unless perdeuteration resulted in a very substantial reduction in the B-to-Q_y radiationless decay rate. We confirm BYZ's observation that the population decay time of the B state of H_2TPP in benzene solution, initially containing ca. 1200 −1300 cm^{-1} of vibrational energy, is ≤50 fs and that the corresponding Q_x fluorescence risetime is ≤100 fs. On the basis of a limited number of trials, we estimate the B-state fluorescence lifetime of TPP-d_{30} in benzene to be ca. 100 fs but cannot obtain a precise value for k_H/k_D owing to the limited temporal resolution of our instrument. Our best estimate is that perdeuteration slows the rate of S_2-S_1 relaxation of H_2TPP by about a factor of 2.

By extrapolating from the comparisons between ZnTPP and ZnTPP-d_{28}, we assume that perdeuteration of the phenyl groups has a negligible effect on the B−Q_y radiationless transition rate of the free base meso-substituted tetraphenylporphine. Thus, any difference between H_2TPP and D_2TPP-d_{28} (if real) must be due to deuteration at the N atoms. Deuteration of the inner periphery at N in H_2TPP and H_2OEP is known to significantly reduce the rate of S_1-S_0 internal conversion (by a factor of almost 6 in D_2TPP), thereby increasing the quantum yield of T_1 in the deuterated compounds.[19] This effect was attributed by Tobita et al.[19] to the change in Franck−Condon factor brought about by lowering the N−H(D) vibrational frequency on deuteration. This is a reasonable explanation given the large $S_1(Q_x)-S_0$ electronic energy gap of 15400 cm^{-1}, but it is unlikely to be the source of a substantial change of Franck−Condon factor at the B−Q_y spacing of ca. 5650 cm^{-1}.

Deuteration at the inner peripheral N atoms in TPP is known to reduce the rate of tunneling along the path leading, ultimately, to its tautomeric structures. If the isotope effect indicated by our limited data is real, tunneling of the H(D) atoms may be responsible for the greatly enhanced B−Q_y coupling observed in the free base porphyrin. Such an interpretation would be consistent with the tunneling model of radiationless transitions developed by Formosinho et al.[20] only if displacement along the N−H(D) but not the C−H(D) stretching coordinates lead to interstate coupling.

(iii) Effect of Electron Configuration and Size of the Metal Atom in Meso-Substituted Tetraphenylmetalloporphyrins. X-ray crystal structures and NMR relaxation studies show that the ground states of some sterically crowded meso-substituted tetraarylmetalloporphyrins have macrocycles that are ruffled or saddle-shaped; that is, the tetrapyrrole framework is nonplanar.[21,22] Moreover, the full metalloporphyrin structure can be distinctly pyramidal when the size of the metal ion (e.g., Cd^{2+}) exceeds that of the cavity provided by the tetrapyrrole ligands or when a solvate ligand such as pyridine pulls the metal ion out of the macrocyclic plane.[23] Although such structural differences may be important in understanding the biophysical functions of the metalloporphyrins and related materials and the effects of nonplanar distortions on electronic spectra have been the source of some controversy,[22] it is not known whether they are important determinants of the photophysical properties of the S_2 states of the d^0 and d^{10} molecules studied here.

We have previously reported[9] detailed analyses of the photophysical behavior of MgTPP and ZnTPP in a wide variety of solvents together with a preliminary measurement of the lifetime of the S_2 state of CdTPP. We have now measured the S_2-decay and S_1-rise times of CdTPP in two solvents with improved temporal resolution *(vide supra)*. The data are summarized in Table 2 and show that the S_2-S_1 internal conversion rates in CdTPP are consistent with the trends established for MgTPP and ZnTPP. That is, (i) S_2-S_1 internal conversion is the major S_2 decay process in all three molecules (i.e., heavy-atom enhanced intersystem crossing is not primarily responsible for the increased rates of radiationless decay in

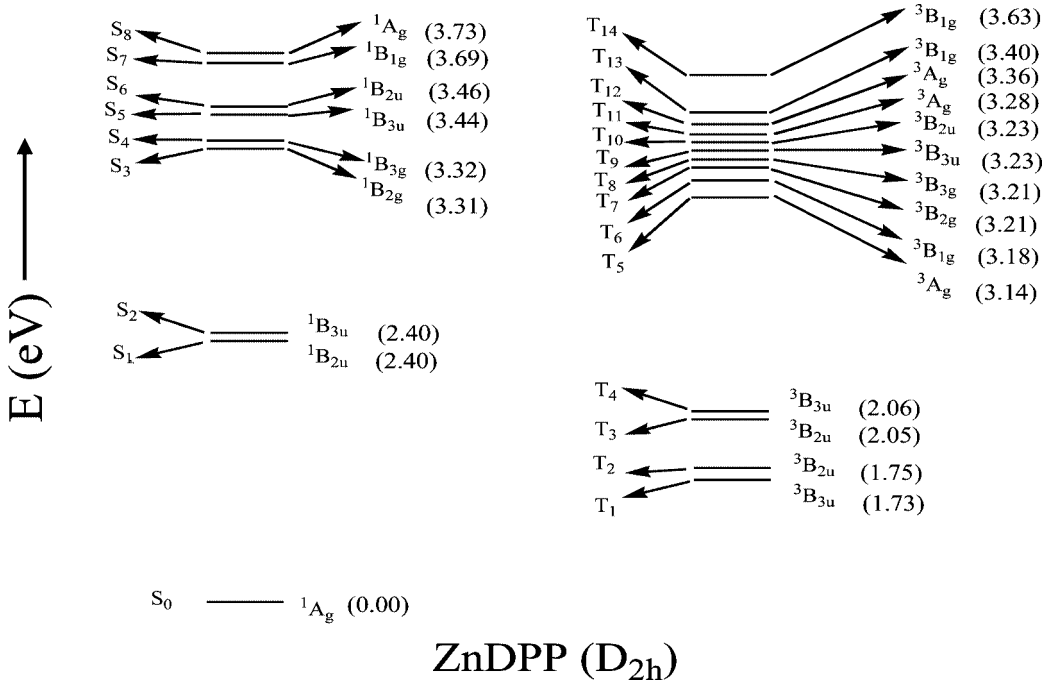

Figure 2. TD-DFT calculations of the ground- and excited-state energies (in eV) of ZnDPP showing lifting of the degeneracies of the E_u and E_g states of ZnTPP. (For ZnTPP data see ref 11.)

ZnTPP and especially CdTPP), (ii) the rate of S_1 population rise is equal to the rate of S_2 population decay within an error limit of ca. 50 fs, (iii) the rate of S_2-S_1 relaxation in CdTPP increases as the solvatochromically controlled energy gap decreases just as it does in MgTPP and ZnTPP, and (iv) the S_2-S_1 interstate coupling energies increase from MgTPP to ZnTPP to CdTPP; MgTPP falls in the weak coupling limit, whereas ZnTPP and especially CdTPP fall in the intermediate coupling range. However, these facts do not speak directly to the source of the increased coupling, in particular the possible effects of the altered metalloporphyrin structure (from planar to pyramidal) when the larger Cd^{2+} ion is complexed in the MTPP series[23] (*vide infra*).

(iv) Effect of a Change in the Symmetry of Meso-Substitution by Phenyl Groups. The S_2 decay and S_1 rise times of ZnTPP (D_{4h} meso-substituted macrocycle symmetry) and ZnDPP (D_{2h} meso-substituted macrocycle symmetry) were compared for purposes of examining the effect of the meso-substitution pattern on the S_2 radiationless relaxation rates. Figure 2 shows the results of TD-DFT calculations on the 5,15-diphenyl-substituted porphyrin that may be compared with previous similar calculations on ZnTPP.[11] These calculations show that each excited electronic state in ZnTPP is split into two closely spaced states ($\Delta E \leq 0.02$ eV) when the symmetry is reduced from D_{4h} to D_{2h}. The S_1 and S_2 states are both of ^1E_u symmetry in ZnTPP, and both are split into states of $^1B_{2u}$ and $^1B_{3u}$ symmetry in the D_{2h} molecule. Although the Soret and Q bands occur at slightly different energies in the two compounds, this splitting results in no substantial effect on the solution phase absorption and emission spectra or in the emission lifetimes. (In the same solvent, the S_2-S_1 electronic energy gap of ZnDPP is about 200 cm^{-1} larger than that in ZnTPP, but the variation in this spacing with f_1 (vide infra) is identical because the solvatochromic shifts in the energies of the S_2 and S_1 states are similar in both compounds.) The measured S_2 radiationless transition rates (inverse of the S_2 lifetimes) and S_1 rise times of the D_{4h} and D_{2h} molecules are similar, as summarized in Table 2.

These results are similar to those found previously by Mataga et al.[14] who measured the temporal S_2 decay and S_1 rise profiles of ZnTPP in ethanol and a zinc meso-diarylporphyrin in tetrahydrofuran (THF). These observations suggest that not only is the aryl-substitution pattern not a significant factor in determining the S_2 decay rates but also that Jahn−Teller instability[24] of the D_{4h} metalloporphyrins generally may not play an important role in determining their S_2 population decay rates. The singlet and triplet states of D_{4h} metalloporphyrins with closed-shell ground states are spatially 2-fold vibronically degenerate. This degeneracy may be lifted both by static means (substitution pattern as is the case with ZnDPP, axial ligation, or nonbonding interactions with solvent) and by dynamic (vibrational) means. The latter, dynamic Jahn−Teller effect arises when nontotally symmetric vibrations lift the degeneracy of ^1E_u states such as S_2, selectively stabilizing one vibronic state and thereby enhancing couplings that otherwise would be weak. None of the data obtained here, including the effects of solvent coordinating ability and macrocycle substitution pattern, suggest that either the static or dynamic Jahn−Teller effects associated with lifting the symmetry of the ^1E_u excited states is an important determinant of the S_2 population decay rates.

(v) Effect of Extensions of the Conjugated Macrocycle Structure and Meso-Tetraphenyl Substitution. To test the possible effects of extensions of the conjugated π-electron macrocycle structure and any incremental distortions from planarity introduced by meso-tetraphenyl substitution, we have examined the relaxation dynamics of Soret-excited ZnP, ZnTBP, and ZnTPTBP (Chart 1) in several solvents and have compared the results with those previously obtained for ZnTPP.[9] The absorption and emission spectra of these compounds in solution have been reported previously.[25−28] The spectra obtained here for ZnP and ZnTPTBP do not differ significantly, but the spectra of ZnTBP require comment. A significant impurity with an absorption maximum near 460 nm has been reported in previous syntheses of ZnTBP and is also present in commercially available samples. The discrepancies in the reported quantum yields of S_2-S_0 fluorescence in this compound have been

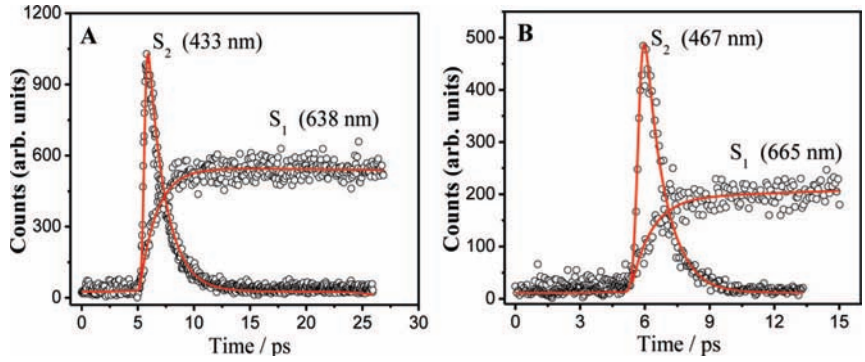

Figure 3. Temporal S_2 and S_1 fluorescence upconversion profiles of (a) ZnTBP in pyridine ($\tau(S_2) = 1.53$ ps; $\tau(S_1$ rise$) = 1.51$ ps) and (b) ZnTPTBP in ethanol ($\tau(S_2) = 930$ fs; $\tau(S_1$ rise$) = 933$ fs). Measurements are at room temperature with $\lambda_{ex} = 400$ nm, and central observation wavelength is shown. The solid lines give the best fits of single-exponential decay and rise functions to the measured data.

attributed to such contamination of this compound.[25,26] Particular care was therefore taken in purifying and characterizing the ZnTBP used in this study; any remaining impurity absorbing at 460 nm in the sample was nonfluorescent. Details are given in the Supporting Information accompanying this paper.

The spectroscopic and excited-state decay rate data for ZnP, ZnTBP, and ZnTPTBP are summarized in Tables 1 and 2. The temporal S_2 fluorescence decay and S_1 fluorescence rise profiles for ZnTBP and ZnTPTBP are shown in Figure 3. Sparing solubilities of these larger metalloporphyrins limited the number of noncoordinating solvents that could usefully be employed in these studies. Nevertheless, distinct differences between the spectroscopic and photophysical behaviors of the two tetrabenzo-substituted compounds, ZnTBP and ZnTPTBP, compared with ZnP or ZnTPP may be observed. Key among their spectroscopic differences are the much larger intrinsic S_2-S_1 electronic energy spacing of ZnTBP, the smaller S_2-S_1 spacing of ZnTPTBP, and the larger relative intensities of the Q bands both compared with ZnP or ZnTPP.[25−28] Note particularly that ZnTBP has an S_2-S_1 energy gap, $\Delta E(S_2-S_1)$, of 8953 cm^{-1} in the cold isolated molecule,[29] about 8400 cm^{-1} in an Ar matrix,[28a] and 7625 cm^{-1} in ethanol, considerably larger than the spacings found for ZnTPP in similar media.

It is revealing to note that if ZnTBP were to exhibit the same energy gap law behavior as that of ZnTPP,[9] its S_2 lifetimes should lie in the 50−500 ps region because of its larger S_2-S_1 electronic energy spacing. However, this is not the case; previous estimates of the S_2 population decay time of Soret-excited ZnTBP are ca. 4 ps (homogeneous line width measurement in a supersonic expansion)[29] and 2.4 ps (from the measured S_2 fluorescence quantum yield and a calculation of the S_2-S_0 radiative decay rate obtained by using the Strickler−Berg method).[27] We measured $\tau_{S2} = 1.01$, 1.30, 1.53, and 2.55 ps in benzene, ethanol, pyridine, and DMF, respectively (cf. Table 2) and calculated a set of radiationless decay constants that are comparable to those found in ZnTPP. For ZnTPTBP, the results are similar, with smaller S_2-S_1 energy spacings yielding lifetimes of $\tau_{S2} = 0.43$, 0.68, 0.74, and 0.93 ps in pyridine, benzene, DMF, and ethanol, respectively, all slightly shorter than those of ZnTBP. For ZnP, the lifetime, $\tau_{S2} = 0.91$ ps in ethanol, is comparable to that of ZnTPTBP despite its significantly larger energy gap ($\Delta E(S_2-S_1) = 7445$ cm^{-1} in ethanol). The data are collected in Tables 1 and 2.

Three conclusions may be drawn from these data. First, by comparing ZnTBP with ZnP, one observes that the effect of extending the conjugated π-electron system on the S_2-S_1 radiationless decay rate cannot be rationalized on the basis of a change in either the S_2-S_1 energy gap or the rigidity of the macrocycle framework. Second, the effect of meso-tetraphenyl substitution of either ZnP to give ZnTPP or of ZnTBP to give ZnTPTBP can also not be correlated with incremental changes in macrocycle geometry, as implied in previous papers.[6] Third, the initial excess vibrational energy content of these porphyrins in solution (E_{vib} increasing from ca. 0 cm^{-1} in ZnP to ca. 3500 cm^{-1} in ZnTPTBP), caused by exciting these metalloporphyrins at the same wavelength (400 nm) as the B-band origin shifts bathochromically with benzo-annulation and phenyl- substitution, has no significant effect on the S_2 dynamics.

(vi) Effect of Halogenation of Meso-Phenyl Groups. Halogenation of metalloporphyrins at either the β-positions or in the meso-phenyl substituents is known to strongly affect the spectroscopic and lower excited-state photophysical properties of both the free-base porphyrins and their metallated derivatives.[22] To investigate the effects of halogenation of the phenyl rings on the S_2 radiationless decay rates of the meso-substituted tetraphenylporphyrins, we have measured the spectroscopic and dynamic behavior of Soret-excited ZnTPP(F_{20}) and ZnTPP(Cl_8) in ethanol and have compared the results with those for ZnTPP. The data are presented in Tables 1 and 2. The effect of perfluorination of the phenyl groups is particularly dramatic and results in a 6-fold increase in the rate of radiationless decay of ZnTPP(F_{20}) compared with ZnTPP at almost the same electronic energy gap. Partial chlorination of the phenyl rings, as exemplified by ZnTPP(Cl_8), has only a small effect on the S_2-S_1 spacing and a correspondingly mild effect on the S_2 radiationless decay rate. In fact, the datum for ZnTPP(Cl_8) falls squarely on the energy gap law correlation for ZnTPP itself. This is an interesting finding because perfluorination results in a withdrawal of electron density from the macrocycle framework and, according to previous convincing interpretations, leads to ruffling of the macrocycle,[22] whereas partial chlorination has no such effect. That is, whereas ZnP and ZnTPP (and presumably ZnTPP(Cl_8)) are planar, ZnTPP(F_{20}) is nonplanar because of relief of strain (in-plane nuclear reorganization, IPNR[22b]) caused by significant changes in bond lengths and bond angles upon perfluorination of the pendant phenyl groups.

Because both ZnTPP and ZnTPP(F_{20}) have similar energy gaps in the same solvent, it would be tempting to ascribe the larger S_2-S_1 radiationless transition rate in the perfluorinated compound compared to the planar perhydro one to these changes in equilibrium conformation. However, as previously shown for perfluoroalkyl porphyrins,[22b] nonplanarity (ruffling) itself is not the source of the bathochromic shifts in the Q bands of the free base porphyrins and their zinc(II) metallated analogues—an analysis that was later confirmed by high-level TDDFT calculations and extended to saddling distortions in the same

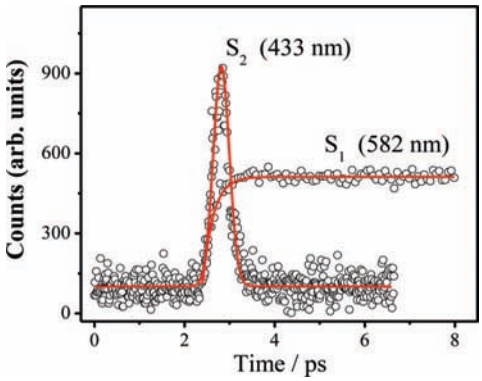

Figure 4. Temporal S_2 and S_1 fluorescence upconversion profiles of ZnOEP in ethanol at room temperature. Measurements are for λ_{ex} = 400 nm and the central observation wavelength shown. For the S_2 fluorescence upconversion signal, the solid line gives the best fit of the data to a Gaussian instrument response function with fwhm = 400 fs and S_2 population decay time, $\tau(S_2)$ = 24 fs. For the S_1 fluorescence signal, the solid line gives the best fit to an S_1 population rise time, $\tau(S_1$ rise) = 30 fs. (See ref 9 for details.)

compounds.[22c] Rather, the substituent-induced red-shifts in the optical spectra of the normal metalloporphyrins and whatever nonplanarity accompanies them are the result of changes in bond lengths and bond angles in the macrocycle skeleton, that is, the in-plane reorganization of the nuclear coordinates as described by DiMagno and co-workers.[22]

(vii) ZnOEP and Other Non-Fluorescent (from S_2) d^0 or d^{10} Metalloporphyrins. The Soret-excited (S_2) state of ZnOEP has been described as non-fluorescent.[30] However, careful steady-state measurements with a spectrofluorometer fitted with double excitation and emission monochromators reveals (after corrected Raman background subtraction) very weak emission in the 400−430 nm range when exciting at wavelengths to the blue of the main Soret band. The location and shape of this band, together with the absence of spurious bands in the S_1-S_0 emission spectrum, rules out potential impurities such as the free base (H_2OEP) as the source of this emission. Precise quantitative measurements were not possible, but the quantum yield of S_2-S_0 fluorescence is estimated to be ca. 1×10^{-6}. A calculation of the S_2-S_0 radiative rate constant from the integrated absorption intensity of the Soret band of ZnOEP together with this quantum yield results in an estimate of the lifetime of the S_2 state of ca. 20 fs and a radiationless decay rate of ca. 5×10^{13} s^{-1}. Nevertheless, because the oscillator strength of the Soret transition in ZnOEP is so large, it is still possible to obtain S_2-S_0 fluorescence of sufficient intensity to measure its temporal fluorescence upconversion decay profile, as well as that of the S_1 fluorescence rise (Figure 4). This profile is almost indistinguishable from the pure Gaussian instrument response function when both are obtained with a 3.3 fs step size during data acquisition, a result that is completely consistent with the calculation of the S_2 lifetime of ca. 20 fs. Note that the 5×10^{13} s^{-1} decay rate is almost exactly the average frequency of the ground-state in-plane C−C and C−N stretching vibrations of the porphyrin macrocycle that are Franck−Condon active in the spectra and are the accepting modes in the S_2-S_1 radiationless decay of ZnTPP.[9]

The following facts concerning the relaxation of Soret-excited ZnOEP are now established. Because the quantum yield of S_1 emission is essentially independent of excitation wavelengths spanning both the Q and B bands, the quantum efficiency of S_2-S_1 internal conversion must be close to 1, just as it is in ZnP and ZnTPP. The S_2-S_1 electronic energy spacing of β-substituted ZnOEP in solvents such as ethanol is slightly larger than that of meso-substituted ZnTPP in the same solvents (Table 1); therefore, an energy gap law argument[31] cannot be used to explain the difference in their radiationless decay rates. Apart from the pendant substituents, ZnOEP, ZnP, and ZnTPP are all planar; therefore, the difference in their decay rates is not related to macrocycle conformation. The amount of vibrational energy deposited in these metalloporphyrins[18] also cannot be an important factor in determining the differences in radiationless decay rates, because the largest amount of vibrational energy is deposited in ZnTPP (E_{vib} = 1350 cm^{-1}) and the least in ZnP (ca. 0 cm^{-1}), compared with ca. 500 cm^{-1} for ZnOEP when exciting at 400 nm.

We conclude that strong S_2-S_1 coupling is present in ZnOEP and therefore attribute its much larger S_2 radiationless decay rate to a larger electronic coupling constant. The source of this strong coupling and whether strong coupling is characteristic of all β-substituted metalloporphyrins is discussed below.

Global Analysis and Conclusions

Several general conclusions may be drawn from analyzing all the S_2 spectroscopic and relaxation data presented above and in the first paper in this series.

First, the major S_2 population decay pathway is S_2-S_1 internal conversion in all molecules. The superimposability of the absorption and the corrected, normalized fluorescence excitation spectra of these metalloporphyrins obtained by exciting in either the Q or B bands and observing Q-band fluorescence indicates that no important excitation wavelength-dependent process is occurring in any of these metalloporphyrins in solution. This conclusion is consistent with the observation that the radiationless decay rates of the S_2 states of these molecules are not a function of their initial vibrational energy content at vibrational energies up to ca. 3500 cm^{-1} (in some compounds). Moreover, the quantum efficiency of S_2-S_1 internal conversion is large, approaching 1.0 in all the systems studied in this paper except CdTPP where it is 0.69.

Second, the rate of S_2 fluorescence decay is equal to the rate of S_1 fluorescence rise (within a measurement error of ca. 50 fs). The temporal S_2 population decay profiles are well-represented by single exponential functions in all compounds examined to date. This observation is in agreement with those of Mataga et al.[14] and Gurzadyan et al.[32] We thus cast some doubt on one previous measurement by Yu et al.,[13] who reported that the rate of decay of the S_2 fluorescence of ZnTPP in benzene was measurably slower than the rate of rise of S_1 fluorescence. In the small number of cases, such as CdTPP[9] and two metallocorroles,[33] in which the quantum efficiency of S_2-S_1 internal conversion is significantly less than 1.0, the S_2 and S_1 decay and rise times remain equal, indicating that any dark state responsible for an internal conversion efficiency of <1.0 in these molecules is populated in a parallel not a sequential S_2 relaxation process.

Third, the S_2-S_1 electronic energy gap plays at least some role in determining the rate of S_2-S_1 internal conversion in most of these d^0 and d^{10} metalloporphyrins. This observation is not new; many groups (including ours) have previously attempted to use energy gap law correlations to rationalize S_2 relaxation rates in these and other similar metalloporphyrins.[9,13,18,31,32,34] The data presented in Tables 1 and 2 do, however, enable us to establish the fundamentals of how the S_2-S_1 gap changes with solvent and macrocycle polarizability and thereby influences the rate of S_2 decay, as we shall discuss below.

We have previously shown[9,11] that the S_2-S_1 energy gap is a linear function of the solvent's Lorenz−Lorentz polarizability

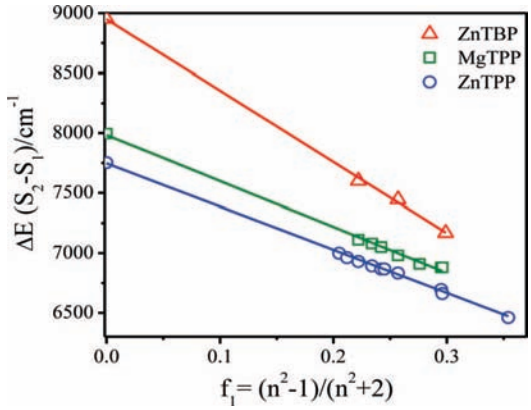

Figure 5. Plots of $\Delta E(S_2-S_1)$ versus the solvent polarizability function $f_1 = (n^2 - 1)/(n^2 + 2)$ for ZnTBP. The data for MgTPP and ZnTPP from ref 9 and the values of $\Delta E(S_2-S_1)$ for the isolated molecules from supersonic jet spectroscopy (refs 29 and 36) are also plotted.

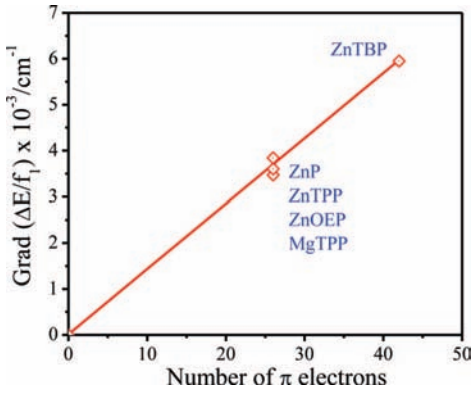

Figure 6. Gradients of $\Delta E(S_2-S_1)$ versus f_1 plots (Figure 4 and other gas-phase data, see text) versus the number of π electrons in the fully conjugated macrocycle framework.

function, $f_1 = (n^2 - 1)/(n^2 + 2)$ where n is the refractive index of the solvent, for both MgTPP and ZnTPP. (This result is similar to that found earlier by Renge[35] for H_2TPP.) In fact, these two plots have almost the same slopes, and both extrapolate well to the values of $\Delta E(S_2-S_1)$ for the isolated molecules (i.e., at $f_1 = 0$) obtained from their fluorescence excitation spectra in supersonic expansions.[36] Fortunately, the fluorescence excitation spectrum of ZnTBP has also been measured in a supersonic expansion,[29] and a similar plot (Figure 5) of $\Delta E(S_2-S_1)$ versus f_1 including the datum for the isolated molecule reveals that the S_2-S_1 energy gap in this extended macrocycle is much more sensitive to changes in solvent polarizability than is ZnTPP itself. The spectra of H_2P, H_2TPP, and ZnOEP have also been measured previously in the gas phase and in a variety of noncoordinating solvents,[37] yielding additional values of $\Delta E(S_2-S_1)$ as a function of f_1. In fact, for the limited data set available, the gradients of plots of $\Delta E(S_2-S_1)$ versus f_1 are almost identical for all metalloporphyrins possessing the same macrocyclic framework, irrespectively of meso-aryl or β-alkyl substitution. The gradient of $\Delta E(S_2-S_1)$ versus f_1 is a linear function of the total number of π electrons in the macrocycle framework and passes through the origin, as shown in Figure 6, if all π electrons, including those on the pyrrole N atoms, are included (i.e., ZnTBP has 42 π electrons, and all others examined here have 26). These observations are consistent with the previous interpretation[9,35] that dispersive interactions control the magnitude of the solvatochromic shifts in the spectroscopically measured energies of both the S_2 and S_1 states, and hence of $\Delta E(S_2-S_1)$, in solution.

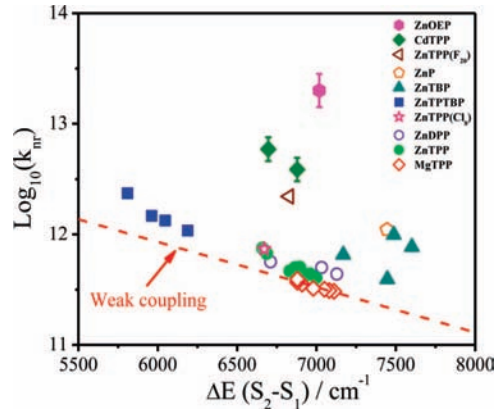

Figure 7. Global analysis of factors controlling the S_2-S_1 internal conversion rate in d^0 and d^{10} metalloporphyrins.

The larger π system of ZnTBP results in proportionally larger polarizabilities of both its S_2 and S_1 states and thus a greater sensitivity of $\Delta E(S_2-S_1)$ to solvent polarizability than that of ZnTPP, MgTPP, and ZnP. Moreover, the meso-substituted phenyl groups play no substantial role in determining the sensitivity of this energy spacing to the strength of dispersive solute−solvent interactions.

Finally, the most important general conclusion to be drawn is that of all the metalloporphyrins examined to date, only MgTPP exhibits S_2 relaxation rates that can properly be described by the weak coupling case of radiationless transition theory and its energy gap law corollary. All of the d^{10} metalloporphyrins, the photophysics of which are described above or in Part I of this series,[9] exhibit S_2-S_1 interactions that are best described by either strong or intermediate coupling. The energy gap law as formulated in the weak coupling case therefore does not apply in general, and the magnitude of $\Delta E(S_2-S_1)$ in some cases is at most a minor controlling factor in determining the S_2-to-S_1 decay rate.

We conclude therefore that when considering different d^0 and d^{10} metallated tetrapyrroles, the magnitude of the S_2-S_1 interstate coupling energy, C, is the most important determinant of the S_2 state's radiationless decay rate. Whether weak or strong coupling[10] is involved, k_{nr} is proportional to C^2, and C needs to vary by a factor of about an order of magnitude to account for the >100-fold difference in radiationless decay rates found for the metalloporphyrins studied here. If we use the weak coupling energy gap law dependence of k_{nr} on $\Delta E(S_2-S_1)$ for MgTPP as a standard[9] and attribute any increase in k_{ic} for other compounds at the same energy gap to a proportionately larger value of C^2, we can then calculate the values of C from the available data. The procedure is illustrated in Figure 7, and the values of C are collected in Table 2. Here, $k_{ic} = \eta_{ic}/\tau_{S2}$, where η_{ic} is taken as 1.0 for all compounds except CdTPP, for which $\eta_{ic} = 0.69$ has been measured.[9] (Note that this ignores the small deviations of η_{ic} from 1.0 measured in some other compounds.) For each metalloporphyrin/solvent pair, the value of k_{ic} associated with weak vibronic coupling is calculated by using the energy gap law correlation for MgTPP at the applicable values of ΔE (Table 2) for which S_2 lifetime measurements have been obtained. That is, the previously determined[9] empirical energy gap law relationship for MgTPP,

$$\log_{10}(k'_{ic}) = 14.38 - 4.1 \times 10^{-4}\Delta E \qquad (3)$$

(where ΔE is in cm^{-1}) is used to obtain k'_{ic} for each metalloporphyrin solvent pair. Such values of k'_{ic} are those that would be found if the metalloporphyrin were to exhibit the same

weak vibronic coupling as MgTPP. The value of C for each compound, X, is then obtained from its measured values of $k_{ic}(X)$ by using

$$k_{ic}(X)/k'_{ic}(X) = (C_X/C_{MgTPP})^2 \quad (4)$$

where the value of C_{MgTPP} is 76 cm^{-1}, as determined previously.[9]

Quantitative evidence for variations in the S_2-S_1 interstate coupling energy may in principle be obtained from the absorption spectra. Ohno et al.[30] have previously shown that for some metalloporphyrins, the ratio of the intensities of the 0−0 and 1−0 bands in the S_1-S_0 (Q) absorption spectra, $\varepsilon_Q(0-0)/\varepsilon_Q(1-0)$, provides a measure of the vibronic B−Q coupling energy. Ohno et al.[30] suggest that the nominally forbidden Q(0−0) band borrows its intensity from the strongly allowed B band when the accidental degeneracy of the $^1(a_{2u}e_g)$ and $^1(a_{1u}e_g)$ excited-state configurations is lifted. (In Gouterman's commonly used four-orbital model,[38] these two configurations interact, with vector summation of the resulting transition moments, to give the separate Q (weak, scalar subtractive) and B (strong, scalar additive) transitions.) They propose[30] that

$$\varepsilon_Q(0-0)/\varepsilon_Q(1-0) = a(\delta E)^2 \quad (5)$$

where δE is the energy difference between the two excited-state electron configurations and a is a constant. The quantity $\varepsilon_Q(0-0)/\varepsilon_Q(1-0)$ is easily measurable from the absorption spectra and is a weak function of the nature of the solvent for a given metalloporphyrin but a relatively strong function of the nature and pattern of the porphyrin's substituents. Data for the compounds investigated here are given in Table 1. If $\Delta E(S_2-S_1)$ for the isolated molecule (obtained by using only the limited data provided by gas phase or supersonic jet measurements) is taken as a measure of δE, $\varepsilon_Q(0-0)/\varepsilon_Q(1-0)$ is seen to be a strong function of the configuration interaction energy (actually much stronger than the quadratic dependence predicted by eq 5). Note, however, that many factors could influence the relative intensities of the 0−0 and 1−0 bands when the data are taken from solution spectra at room temperature. In particular, as for pyrene, naphthalene, and benzene, the Ham effect[39] will be operative in those D_{4h} metallopyrroles the Q bands of which are weak (and pseudoforbidden) because of offsetting transition moments. The origin of the Q-band system will be allowed, however, if the metalloporphyrin loses its center of symmetry−when significantly nonplanar, for example.

A second feature of the absorption spectra that could be correlated with the S_2-S_1 coupling energy is the fraction of the total oscillator strength of the Q−X and B−X transitions that resides in the Q−X transition, $f_Q/(f_Q + f_B)$, which can be obtained from the integrated absorbances of the two band systems.[40] Such data will be less strongly influenced by the overlapping band structure characteristic of spectra taken in solution at room temperature. Again, these data (Table 1) exhibit a relatively weak dependence on solvent (for at least noncoordinating solvents) and a stronger dependence on the metalloporphyrin substitution pattern.

In seeking a correlation between the nonradiative decay rates of the entire set of Soret-excited compounds and $\varepsilon_Q(0-0)/\varepsilon_Q(1-0)$ and/or $f_Q/(f_Q + f_B)$, we plotted $\log(C_X)$ versus $\log[\varepsilon_Q(0-0)/\varepsilon_Q(1-0)]$ and versus $\log[f_Q/(f_Q + f_B)]$ to determine the power dependence of C_X on each quantity. Although C_X tends to increase with both $\varepsilon_Q(0-0)/\varepsilon_Q(1-0)$ and $f_Q/(f_Q + f_B)$ when considering a limited set of similar compounds, both correlations are poor when data for the entire set of metalloporphyrins are included. Consider for example the data for ZnOEP and ZnTBP where the values of C^2 differ by a factor of about 100, whereas the values of $\varepsilon_Q(0-0)/\varepsilon_Q(1-0)$ are almost identical and those of $f_Q/(f_Q + f_B)$ differ by no more than a factor of 5. Thus, the correlation between $\varepsilon_Q(0-0)/\varepsilon_Q(1-0)$ and $(\delta E)^2$ proposed by Ohno et al.[30] does not extend to a correlation between $\varepsilon_Q(0-0)/\varepsilon_Q(1-0)$ and C_X^2 when the data for the entire set of metalloporphyrins are considered.

Finally, Hochstrasser[41] has shown that the bandwidths of electronic transitions can be used as an approximate measure of the vibronic coupling energy between electronic states. For the fwhm of an electronic absorption band involving a transition to a higher electronic excited-state vibronically coupled to a lower excited-state, he derives

$$\Delta E_{1/2} = E_v^2 F\rho \quad (6)$$

where E_v is the vibronic coupling energy defined for each normal mode that has the proper symmetry to allow the two states to interact, F is the Franck−Condon factor, and ρ is the density of vibronic accepting states. This approach can be easily adapted to the absorption spectra of metalloporphyrins by considering the fwhm of the main Soret absorption band and noting that gerade vibrations will be effective in these cases because both interacting states are of ^1E_u symmetry (in D_{4h}). At the same electronic energy gap and for the same macrocycle, F and ρ will be approximately constant, and under these circumstances, the fwhm of the main Soret band should be a measure of E_v^2, to the extent that vibronic coupling is responsible for the spectral broadening.

In solution at room temperature, however, the bands in the absorption spectra are inhomogeneously broadened and quasi-Gaussian in shape rather than the Lorentzian band shapes that are appropriate for application of Hochstrasser's theory.[41] Nevertheless, the ratios of the full widths at half maximum of the Soret bands of the metalloporphyrins to that of MgTPP (weak coupling) might reasonably be expected to scale as the ratios of the squares of the interstate coupling energies, if vibronic coupling is the dominant mode of interaction. The fwhm of the Soret bands do increase qualitatively with increasing C^2, but the predicted correlation between the ratios of the fwhm of the B bands to the ratios of C^2 is not found. The absence of a good correlation between any single spectroscopic observable and C^2 therefore suggests that none of the vibronic coupling models employed in these correlations is appropriate. Direct electronic interaction between the two coupled states, both of which are of ^1E_u symmetry (in D_{4h}), is indicated.

One solution phase spectroscopic observable that might signal the magnitude of direct S_2-S_1 coupling is the difference in the Stokes shifts of the B- and Q-band radiative transitions. (See Table 2 for Stokes shift, SS, data.) If the Stokes shifts were similar for the two bands, this would indicate that the two upper state surfaces are displaced by similar amounts relative to the ground state; if the Stokes shifts were dissimilar, one excited state would be expected to be displaced more than the other, a situation that could lead to increased direct interaction at vibrational energies in S_1 near the zero-point energy of S_2. Such a qualitative trend is observed in the data of Table 1. Unfortunately however, it is not possible to obtain accurate measures of the Stokes shifts from spectra taken in fluid solution at room temperature. The B- and Q-band Stokes shifts of the rigid, more highly fluorescent metalloporphyrins are small (ca. 100−200 cm^{-1}) in comparison with the widths of the bands, and the differences between them are smaller still. The Stokes shifts obtained from the steady-state spectra of the weakly fluorescent (from S_2) molecules are considerably larger but are subject to much greater error. In addition, the B-band Stokes

shifts of the most weakly fluorescent compounds will be somewhat time-dependent because the time scales of intramolecular vibrational relaxation and interstate population decay are comparable. We conclude that only a qualitative correlation between C^2 and the Stokes shifts obtained from steady state solution spectra is possible in these systems.

Finally, we can summarize the trends found in the data gathered in this study. There is no single solution-phase spectroscopic observable that can be readily correlated with the rates of S_2 radiationless decay. Nevertheless, the following trends can be seen. First, the extent of β-alkyl substitution has the effect of increasing the magnitude of S_2-S_1 coupling. β-Octaalkyl porphyrins exhibit strong coupling with S_2 lifetimes equal to macrocycle stretching frequencies. Conical intersection of the S_2 and S_1 states is likely. Second, meso-aryl substitution has the effect of reducing the S_2-S_1 electronic energy spacing somewhat but also reducing the S_2-S_1 coupling energy. The pattern of meso-aryl substitution has little effect. Compounds that have both β-alkyl and meso-aryl substitution exhibit intermediate coupling energies. (Note in this regard Akimoto et al.[42] who report an S_2 population decay time of 150 fs for a β-tetraethyl-meso-diaryl-substituted zinc porphyrin; its value of $C = 315$ cm^{-1} calculated as described above falls squarely in the intermediate coupling regime.) Third, nonplanar tetrapyrroles such as ZnTPP(F_{20}), CdTPP, and the metallocorroles[33] exhibit larger interstate coupling energies than their planar counterparts. We note, however, that nonplanarity may not of itself be the source of increased coupling, as described in detail by DiMagno.[22] Fourth, benzo-annulation of the pyrrole rings increases the polarizability of the excited states in proportion to the number of π electrons in the extended macrocycle and increases the intrinsic S_2-S_1 electronic energy spacing but also increases the sensitivity of the S_2-S_1 spacing to narrowing by dispersive solvatochromic interactions.

Acknowledgment. The authors gratefully acknowledge the continuing financial support of this research program by the Natural Sciences and Research Council of Canada. Support for this project from a FABLS/ARC/NHMRC Network Award RN0460002 and the Australian Research Council's Discovery Project DP0878220 is also acknowledged. The femtosecond fluorescence upconversion facilities were provided through the Saskatchewan Structural Sciences Centre, funded by the Canada Foundation for Innovation, the Province of Saskatchewan, and the University of Saskatchewan. We also thank Dr. Sophie Brunet for her assistance with training and laser maintenance and Dr. Clint P. Woodward for his help in preparing and purifying some of the compounds.

Supporting Information Available: The Supporting Information for this paper contains detailed descriptions of the syntheses of compounds not available commercially and of the purification of ZnTBP. Absorption and emission spectra of representative compounds are also provided. This material is available free of charge via the Internet at http://pubs.acs.org.

References and Notes

(1) (a) Campbell, W. M.; Jolley, K. W.; Wagner, P.; Wagner, K.; Walsh, P. J.; Gordon, K. C.; Schmidt-Mende, L.; Nazeeruddin, M. K.; Wang, Q.; Grätzel, M.; Officer, D. L. *J. Phys. Chem. C* **2008**, *111*, 11760. (b) Steer, R. P. *J. Appl. Phys.* **2007**, *102*, 076102–1. (c) Bell, T. D. M.; Ghiggino, K. P.; Haynes, A.; Langford, S. J.; Woodward, C. P. *J. Porphyrins Phthalocyanines* **2007**, *11*, 455. (d) Tanaka, M.; Hayashi, S.; Eu, S.; Umeyama, T.; Matano, Y.; Imahori, H. *Chem. Commun.* **2007**, 2069. (e) Wang, Q.; Campbell, W. M.; Bonfantani, E. E.; Jolley, K. W.; Officer, D. L.; Walsh, P. J.; Gordon, K.; Humphry-Baker, R.; Nazeeruddin, M. K.; Grätzel, M. *J. Phys. Chem. B* **2005**, *109*, 15397.

(2) (a) Neagu, M.; Manda, G.; Constantin, C.; Radu, E.; Ion, R-M. *J. Porphyrins Phthalocyanines* **2007**, *11*, 58. (b) Mathai, S.; Smith, T. A.; Ghiggino, K. P. *Photochem. Photobiol. Sci.* **2007**, *6*, 995. (c) Nyman, E. S.; Hynninen, P. H. *J. Photochem. Photobiol. B* **2004**, *73*, 1. (d) Pandey, S. K.; Gryshuk, A. L.; Graham, A.; Ohkubo, K.; Fukuzumi, S.; Dobhal, M. P.; Zeng, G.; Ou, Z.; Zhan, R.; Kadish, K. M.; Oseroff, A.; Ranaprasad, S.; Pandey, R. K. *Tetrahedron* **2003**, *59*, 10059.

(3) (a) Gulino, A.; Giuffrida, S.; Mineo, P.; Purrazzo, M.; Scamporrino, E.; Ventimiglia, G.; van der Boom, M. E.; Fragala, I. *J. Phys. Chem. B* **2006**, *111*, 16781. (b) Köse, M. E.; Carroll, B. F.; Schanze, K. S. *Langmuir* **2005**, *21*, 9121. (c) Vinogradov, S. A.; Wilson, D. F. *J. Chem. Soc. Perkin Trans. 2* **1995**, 103.

(4) (a) Pérez-Inestrosa, E.; Montenegro, J-M.; Collado, D.; Suau, R.; Casado, J. *J. Phys. Chem. C* **2007**, *111*, 6904. (b) Remacle, F.; Weinkauf, R.; Levine, R. D. *J. Phys. Chem. A* **2006**, *110*, 177. (c) Yeow, E. K. L.; Steer, R. P. *Chem. Phys. Lett.* **2003**, *377*, 391.

(5) For reviews see: (a) Harvey, P. D.; Stern, C.; Gros, C. P.; Guilard, R. *Coord. Chem. Rev.* **2007**, *251*, 401. (b) Scandola, F.; Chiorboli, C.; Prodi, A.; Iengo, E.; Alessio, E. *Coord. Chem. Rev.* **2006**, *250*, 1471. (c) Ogawa, K.; Yoshiaki, K. *J. Photochem. Photobiol. C.* **2006**, *7*, 1. (d) Takagi, S.; Inoue, H. In *Molecular and Supramolecular Photochemistry*; Ramamurthy, V., Schantze, K. S., Eds.; Marcel Dekker: New York, 2000; Vol. 5, p 215.

(6) For reviews see: (a) Tripathy, U.; Steer, R. P. *J. Porphyrins Phthalocyanines* **2007**, *11*, 228. (b) Burdzinsk, G.; Kubicki, J.; Maciejewski, A.; Steer, R. P.; Velate, S.; Yeow, E. K. L. In *Organic Photochemistry and Photophysics*; Ramamurthy, V., Schantze, K. S., Eds.; Marcel Dekker: New York, 2005; Vol. 14, p 1.

(7) Nappa, M.; Valentine, J. S. *J. Am. Chem. Soc.* **1978**, *100*, 5075.

(8) Sorges, S.; Poisson, L.; Raffael, K.; Krim, L.; Soep, B.; Shafizadeh, N. *J. Chem. Phys.* **2006**, *124*, 114302–1.

(9) Tripathy, U.; Kowalska, D.; Liu, X.; Velate, S.; Steer, R. P. *J. Phys. Chem. A* **2008**, *112*, 5824.

(10) Englman, R.; Jortner, J. *Mol. Phys.* **1970**, *18*, 145.

(11) Liu, X.; Yeow, E. K. Y.; Velate, S.; Steer, R. P. *Phys. Chem. Chem. Phys.* **2006**, *8*, 1298.

(12) (a) Lukaszewicz, A.; Karolczak, J.; Kowalska, D.; Maciejewski, A.; Ziolek, M.; Steer, R. P. *Chem. Phys.* **2007**, *331*, 359. (b) Karolczak, J.; Kowalska, D.; Lukaszewicz, A.; Maciejewski, A.; Steer, R. P. *J. Phys. Chem. A* **2004**, *108*, 4570.

(13) Yu, H-Z.; Baskin, S.; Zewail, A. H. *J. Phys. Chem. A* **2002**, *106*, 9845.

(14) Mataga, N.; Shibata, Y.; Chosrowjan, H.; Yoshida, N.; Osuka, A. *J. Phys. Chem. B* **2000**, *104*, 4001.

(15) (a) Andersson, L. A.; Loehr, T. M.; Thompson, R. G.; Strauss, S. H. *Inorg. Chem.* **1990**, *29*, 2142. (b) Stein, P.; Ulman, A.; Spiro, T. G. *J. Phys. Chem.* **1984**, *88*, 369.

(16) Vacha, M.; Machida, S.; Horie, K. *J. Lumin.* **1995**, *64*, 115.

(17) Zhong, Q.; Wang, Z.; Liu, Y.; Zhu, Q.; Kong, F. *J. Chem. Phys.* **1996**, *105*, 5377.

(18) Baskin, J. S.; Yu, H-Z.; Zewail, A. H. *J. Phys. Chem. A* **2002**, *106*, 9837.

(19) Tobita, S.; Kajii, Y.; Tanaka, I. Porphyrins: Excited States and Dynamics. *ACS Symp. Ser.* **1986**, *321*, 219.

(20) Azhena, E. G.; Serra, A. C.; Pineiro, M.; Periera, M. M.; Seixas de Melo, J.; Arnaut, L. G.; Formosinho, S. J.; Gonsalves, A. M. d'A. R. *Chem. Phys.* **2002**, *280*, 177.

(21) (a) Fleisher, E. B.; Miller, C. K.; Webb, L. E. *J. Am. Chem. Soc.* **1963**, *86*, 2343. (b) Scheidt, W. R.; Kastner, M. E.; Hatano, K. *Inorg. Chem.* **1978**, *17*, 706. (c) Jacobsen, H. J.; Ellis, P. D.; Inners, R. R.; Jensen, C. F. *J. Am. Chem. Soc.* **1982**, *104*, 7442. (d) Scheidt, W. R.; Mondal, J. U.; Eigenbrot, C. W.; Alder, A.; Radonovitch, L. J. *Inorg. Chem.* **1986**, *25*, 795. (e) Cheng, R-J.; Chen, Y-R.; Chuang, E-R. *Heterocycles* **1992**, *34*, 1. (f) Cheng, R-J.; Chen, Y-R.; Chen, C-C. *Heterocycles* **1994**, *38*, 1465.

(22) (a) DiMagno, S. G.; Wertsching, A. K.; Ross II, C. R. *J. Am. Chem. Soc.* **1995**, *117*, 8279. (b) Wertsching, A. K.; Koch, A. S.; DiMagno, S. G. *J. Am. Chem. Soc.* **2001**, *123*, 3932. (c) Ryeng, H.; Ghosh, A. *J. Am. Chem. Soc.* **2002**, *124*, 8099.

(23) (a) Ellis, P. D.; Inners, R. R.; Jakobsen, H. J. *J. Phys. Chem.* **1982**, *86*, 1506. (b) Hazell, A. *Acta Cryst. C* **1986**, *42*, 296. (c) Wun, W-S.; Chen, J-H.; Wang, S-S.; Tung, J-Y.; Liao, F-L.; Wang, S-L.; Hwang, L-P.; Elango, S. *Inorg. Chem. Commun.* **2004**, *7*, 1233.

(24) Hoffman, B. M.; Ratner, M. A. *Mol. Phys.* **1978**, *35*, 901.

(25) Edwards, L.; Gouterman, M.; Rose, C. B. *J. Am. Chem. Soc.* **1976**, *98*, 7638.

(26) Fielding, P. E.; Mau, A.W.-H. *Aust. J. Chem.* **1976**, *29*, 933.

(27) Aaviksoo, J.; Freiberg, A.; Savikhin, S.; Stelmakh, G. F.; Tsvirko, M. P. *Chem. Phys. Lett.* **1984**, *111*, 275.

(28) (a) VanCott, T. C.; Koralewski, M.; Metcalf, D. H.; Schatz, P. N.; Williamson, B. E. *J. Phys. Chem.* **1993**, *97*, 7417. (b) Berezin, D. S.; Toldina, O. V.; Kudrik, E. V. *Russ. J. Gen. Chem.* **2003**, *73*, 1309. (c) Rogers, J. E.; Hguyen, K. A.; Hufnagle, D. C.; McLean, D. G.; Su, W.; Gossett, K. M.; Burke, A. R.; Vinogradov, S. A.; Pachter, R.; Fleitz, P. A. *J. Chem. Phys.* **2003**, *107*, 11331.

(29) Even, U.; Magen, J.; Jortner, J. *J. Chem. Phys.* **1982**, *77*, 4384.
(30) Ohno, O.; Kaizu, Y.; Kobayashi, H. *J. Chem. Phys.* **1985**, *82*, 1779.
(31) Velate, S.; Liu, X.; Steer, R. P. *Chem. Phys. Lett.* **2006**, *427*–295.

(32) (a) Gurzadyan, G. G.; Tran-Thi, T.-H.; Gustavsson, T. *J. Chem. Phys.* **1998**, *108*, 385. (b) Gurzadyan, G. G.; Tran-Thi, T. H.; Gustavsson, T. *Proc. SPIE* **2000**, *4060*, 96.

(33) Liu, X.; Mahammed, A.; Tripathy, U.; Gross, Z.; Steer, R. P. *Chem. Phys. Lett.* **2008**, in press.

(34) Kurabayashi, Y.; Kikuchi, K.; Kokubun, H.; Kaizu, Y.; Kobayashi, H. *J. Phys. Chem.* **1984**, *88*, 1308.
(35) Renge, I. *Chem. Phys. Lett.* **1991**, *185*, 231.
(36) (a) Even, U.; Magen, Y.; Jortner, J. *J. Chem. Phys.* **1982**, *76*, 5684. (b) Even, U.; Magen, J.; Jortner, J.; Friedman, J.; Levanon, H. *J. Chem. Phys.* **1982**, *77*, 4374.

(37) (a) Gale, R.; McCaffery, A. J.; Rowe, M. D. *J. Chem. Soc. Dalton* **1972**, 596. (b) Canters, G. W.; van Egmond, J.; Schaafsma, T. J.; Chan, I. Y.; van Dorp, W. G.; van der Waals, J. H. *Ann. N. Y. Acad. Sci.* **1973**, *206*, 711. (c) Chien, J. C. W. *J. Am. Chem. Soc.* **1978**, *100*, 1310. (d) Davis, W.; Calongne, S.; Rodriguez, J. *J. Chem. Phys.* **1995**, *102*, 716. (e) Starukhin, A.; Shulga, A.; Waluk, J. *Chem. Phys. Lett.* **1997**, *272*, 405. (f) Demchuk, Y. S. *Opt. Spectrosc.* **2004**, *96*, 57.
(38) Gouterman, M. In *The Porphyrins*; Dolphin, D., Ed.; Academic Press: New York, 1978; Vol. III, p 1.
(39) Nakajima, A. *Bull. Chem. Soc. Jpn.* **1971**, *44*, 3272.
(40) (a) Siebrand, W. *Chem. Phys. Lett.* **1971**, *9*, 157. (b) Orlandi, G.; Siebrand, W. *J. Chem. Phys.* **1973**, *58*, 4513.
(41) Hochstrasser, R. M. *Acc. Chem. Res.* **1968**, *1*, 266.
(42) Akimoto, S.; Yamazaki, T.; Yamazaki, I.; Osuka, A. *Chem. Phys. Lett.* **1999**, *309*, 177.

JP804792X